Unified generation and fast emission of arbitrary single-photon multimode W states

Juncong Zheng,[1] Jie Peng [1,*] Pinghua Tang,[1,†] Fei Li,[2] and Na Tan[3]

[1]*Hunan Key Laboratory for Micro-Nano Energy Materials and Devices,*
and School of Physics and Optoelectronics, Xiangtan University, Hunan 411105, China
[2]*Department of Physics, Hunan First Normal University, Changsha 410205, China*
[3]*Department of Fundamental courses, PLA Army Special Operations Academy, Guilin, 541002, China*

We propose a unified and deterministic scheme to generate arbitrary single-photon multimode W states in circuit QED. A three-level system (qutrit) is driven by a pump-laser pulse and coupled to N spatially separated resonators. The coupling strength for each spatial mode g_i totally decide the generated single-photon N-mode W state $|W_N\rangle = \frac{1}{A} \sum_{i=1}^{N} g_i |0_1 0_2 \cdots 1_i 0_{i+1} \cdots 0_N\rangle$, so arbitrary $|W_N\rangle$ can be generated inside resonators by adjusting g_i and N. Moreover, such W states can be fast emitted in symmetric temporal waveform with a probability reaching 98.9%. The generation (or emission) time and fidelity can both be the same for arbitrary $|W_N\rangle$, independent of mode numbers. Finally, the time evolution process is easy to control since only the pump pulse is time-dependent.

I. INTRODUCTION

Entanglement is essential to quantum information, which is widely applied in quantum dense coding [1], quantum teleportation [2], quantum cryptography [3], and quantum computing [4]. It was first proposed by Einstein, Podolsky, and Rosen (EPR) to challenge the completeness of quantum mechanics [5]. There are two inequivalent categories of tripartite entanglement state [6], the Greenberger-Horne-Zeilinger (GHZ) state [7–10] and the W state [11], which could be used to prove Bell's theorem without inequalities [12]. Notably, the W state is more robust than the GHZ state since if one particle is traced out, it retains multiparticle entanglement [12]. Extended to the multipartite case, the general form of a W state is [13,14]

$$|W_N\rangle = \frac{1}{A} \sum_{i=1}^{N} A_i |0_1 0_2 \cdots 1_i 0_{i+1} \cdots 0_N\rangle, \qquad (1)$$

where $A = (\sum A_i^2)^{1/2}$. $|1\rangle$ and $|0\rangle$ represent two orthogonal states encoded in frequencies [15,16], polarizations [17–19], or spatial modes [20–22] of photons, or qubit energy state [23–25].

Various schemes for preparing W states have been proposed, via spontaneous four-wave mixing [15,16], polarizing beam splitter (PBS) [17–19], cavity QED [24–26], circuit QED [13,22,27–30], cold neutral atoms [31], spin system [32] and so on. One interesting kind among them is called "chiral W states" [33,34], which can be used in a noiseless-subsystem qubit encoding, and have recently been realized theoretically with trapped ions by Cole *et al.* [33]. However, a unified

scheme to generate arbitrary W states with high fidelity, speed, and feasibility is needed. First, W states are useful from lower-order to higher-order, since the later establishes entanglement between a large number of channels, making them favorable for realization of quantum information process. For example, Gottesman *et al.* has shown this state is beneficial in longer baseline telescopes [35]. However, the preparation of higher-order W states often involves complex bulk-optical setups [36–38], and the scheme is complex. Second, the coefficient of each basis needs to be easily tunable, because sometimes we require not only the maximum entangled W state where all A_i are equal [39], but also some other types. For example, the prototype W state $|W_3\rangle = \frac{1}{\sqrt{3}}(|100\rangle + |010\rangle + |001\rangle)$ is not suitable for quantum teleportation [40], while another one $|W_3'\rangle = \frac{1}{2}(|100\rangle + |010\rangle + \sqrt{2}|001\rangle)$ proposed by Agrawal and Pati is perfect for teleportation and superdense coding [41,42]. It has been demonstrated that different W states can be transformed by entanglement concentration [43,44], but the process is complex. Third, states must be generated with high speed and fidelity to accelerate the operation and avoid decoherence in practical quantum information processing. Finally, the scheme should be easy to realize with high experimental feasibility.

In this paper, we present a unified deterministic scheme to generate arbitrary single-photon multimode W states $|W_N\rangle$, satisfying the aforementioned requirements. We have a qutrit [45] [e.g., a Λ-type superconducting quantum interference device (SQUID) [46,47], transmon [48–50], Xmon [51], or fluxoniums [52,53]] driven by a pump-laser pulse and coupled to N spatially separated resonators, to obtain $|W_N\rangle$ (1) with A_i equaling the coupling strength between the ith resonator mode and the qutrit g_i. Hence we can generate arbitrary W state by adjusting g_i and N. We can not only create $|W_N\rangle$ inside resonators through adiabatic evolution along a dark state

---

*[*]jpeng@xtu.edu.cn
*[†]pinghuatang@xtu.edu.cn
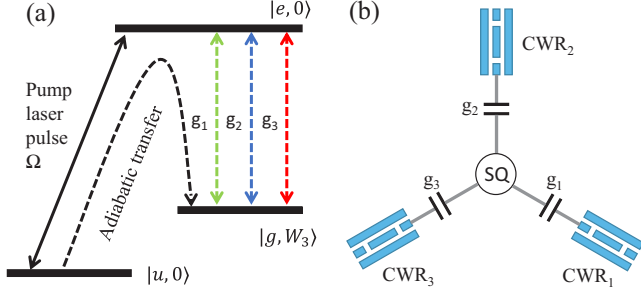
FIG. 1. Scheme of generating the three-mode single-photon W state $|W_3\rangle$ inside resonators through adiabatic passage. (a) Relevant energy levels and transitions. The qutrit states are labeled by $|u\rangle$, $|e\rangle$, and $|g\rangle$. $|0\rangle$ and $|1\rangle$ denote the photon number states in the resonator. (b) Setup: a superconducting qutrit (SQ) is capacitively coupled to three coplanar waveguide resonators (CWRs) with coupling strength g_1, g_2, g_3, and a pump laser pulse with Rabi frequency Ω.

but also emit it into transmission lines through dissipation with symmetric temporal profile, in favor of its reabsorption by quantum nodes. The emission probabilities reach 98.9% in 20–50 ns depending on parameters, comparable to the fastest two-qubit gate (30–45 ns) recently reported [54]. The generation (or emission) time and fidelity (or probability) can both be the same for arbitrary $|W_N\rangle$, independent of mode numbers. Besides, we only need to tune the pump pulse during the whole time evolution process, which is easier to control than the qutrit and resonators.

II. GENERATING THE SINGLE-PHOTON THREE-MODE W STATE INSIDE RESONATORS

Although we aim to generate arbitrary N-mode W state, we start with the prototype three-mode case, with our our scheme depicted in Fig. 1. The qutrit has a Λ-type configuration formed by two lowest levels $|u\rangle$, $|g\rangle$ and an excited level $|e\rangle$. The resonator states are denoted by $|n\rangle$, where n is the number of photons. Their frequencies are identical and far off resonance from the $|e\rangle$ to $|u\rangle$ transition, so their interactions with the qutrit only couple $|e, n\rangle$ and $|g, n+1\rangle$ with coupling strengths g_1, g_2, and g_3, respectively. A pump laser pulse with Rabi frequency Ω only couples $|e, n\rangle$ to $|u, n\rangle$ for the same reason, as shown in Fig. 1. The system is initially in $|u, 0\rangle$ and evolved into $|g, W_3\rangle$ through a stimulated Raman adiabatic passage (STIRAP) along a dark state.

In the one-photon manifold $\{|u, 000\rangle, |e, 000\rangle, |g, 100\rangle, |g, 010\rangle, |g, 001\rangle\}$ under rotating wave approximation (RWA), the Hamiltonian reads ($\hbar = 1$) [55,56]

$$H = \sum_{i=u,e} E_i|i, 000\rangle\langle i, 000| + (E_g + \omega)(|g, 100\rangle\langle g, 100|$$
$$+ |g, 010\rangle\langle g, 010| + |g, 001\rangle\langle g, 001|)$$
$$+ \left[\frac{1}{2}\Omega e^{-i\omega_P t}|e, 000\rangle\langle u, 000| + g_1|e, 000\rangle\langle g, 100|\right.$$
$$\left.+ g_2|e, 000\rangle\langle g, 010| + g_3|e, 000\rangle\langle g, 001| + \text{H.c.}\right], \quad (2)$$

where E_i represents the eigenvalue of the ith energy level, ω is the frequency of each resonator. ω_P is the frequency of the pump pulse.

In the interaction picture with respect to free Hamiltonian

$$H_0 = E_u|u, 000\rangle\langle u, 000| + (E_u + \omega_p)|e, 000\rangle\langle e, 000|$$
$$+ (E_u + \omega_p)(|g, 100\rangle\langle g, 100| + |g, 010\rangle\langle g, 010|$$
$$+ |g, 001\rangle\langle g, 001|), \quad (3)$$

the interaction Hamiltonian reads

$$\frac{1}{2}\begin{pmatrix} 0 & \Omega & 0 & 0 & 0 \\ \Omega^* & 2\Delta_1 & 2g_1 & 2g_2 & 2g_3 \\ 0 & 2g_1^* & 2(\Delta_1 - \Delta_2) & 0 & 0 \\ 0 & 2g_2^* & 0 & 2(\Delta_1 - \Delta_2) & 0 \\ 0 & 2g_3^* & 0 & 0 & 2(\Delta_1 - \Delta_2) \end{pmatrix},$$
$$(4)$$

where $\Delta_1 = (E_e - E_u) - \omega_p$ and $\Delta_2 = (E_e - E_g) - \omega$ are the detunings of atomic transition from the pump pulse and cavities, respectively. Under the two-photon resonance condition $(\Delta_1 = \Delta_2)$ [55,57], there are three degenerate dark states $\{2g_1|u, 000\rangle - \Omega|g, 100\rangle, 2g_2|u, 000\rangle - \Omega|g, 010\rangle, 2g_3|u, 000\rangle - \Omega|g, 001\rangle\}$ with constant eigenergy $E_0 = 0$, so a general solution with $E_0 = 0$ reads

$$|\Psi_0\rangle = \frac{1}{\mathcal{N}}\left[2\sum_{i=1}^{3} A_i g_i|u, 000\rangle - \Omega A|g, W_3\rangle\right], \quad (5)$$

where $A = (\sum_{i=1}^{3} A_i^2)^{1/2}$, $|g, W_3\rangle = |g\rangle \otimes |W_3\rangle$, $|W_3\rangle = \frac{1}{A}(A_1|100\rangle + A_2|010\rangle + A_3|001\rangle)$, and $\mathcal{N} = [4(\sum_{i=1}^{3} A_i g_i)^2 + \Omega^2 A^2]^{1/2}$ is the normalizing constant. The coefficients of $|g, 100\rangle$, $|g, 010\rangle$, and $|g, 001\rangle$ in Eq. (5) are ΩA_i $(i = 1, 2, 3)$, respectively. According to the Schrödinger equation $i\hbar\frac{\partial\psi}{\partial t} = H\psi$, we obtain $\frac{d\Omega A_i}{dt} = -ig_i c_e$, where $c_e = \langle e, 000|\psi\rangle$. Meanwhile, the proposed initial state is $|u, 000\rangle$, which means $\Omega A_i(t = 0) = 0$. Therefore $A_1 : A_2 : A_3 = g_1 : g_2 : g_3$ in this specific case, and Eq. (5) is simplified as

$$|\Psi_0\rangle = \frac{1}{\sqrt{4A^2 + \Omega^2}}[2A|u, 000\rangle - \Omega|g, W_3\rangle], \quad (6)$$

where $A = (\sum_{i=1}^{3} g_i^2)^{1/2}$, and $|W_3\rangle = \frac{1}{A}(g_1|100\rangle + g_2|010\rangle + g_3|001\rangle)$. The other two bright eigenstates to H (4) can be written in terms of the above A and $|W_3\rangle$ as

$$|\Psi_\pm\rangle = \frac{1}{\mathcal{N}_\pm}[\Omega|u, 000\rangle + 2A|g, W_3\rangle$$
$$+ (\Delta_1 \pm \sqrt{4A^2 + \Delta_1^2 + \Omega^2})|e, 000\rangle], \quad (7)$$

with $E_\pm = [\Delta_1 \pm (4A^2 + \Delta_1^2 + \Omega^2)^{1/2}]/2$ respectively, where $\mathcal{N}_\pm = \{2[4A^2 + \Omega^2 + \Delta_1^2 \pm \Delta_1(4A^2 + \Omega^2 + \Delta_1^2)^{1/2}]\}^{1/2}$ is the normalizing constant. Since g_i is adjustable, the dark state $|\Psi_0\rangle$ can be used to generate arbitrary single-photon three-mode W states inside resonators. First we set $g_1 : g_2 : g_3$ on demand, and then turn on the pump pulse which rises slowly enough to ensure the adiabatic transfer from $|u, 000\rangle$ to $|g\rangle \otimes |W_3\rangle$ when $\Omega \gg g_i$. Choosing the pump pulse $\Omega = \Omega_0 \exp[-(t - \tau)^2/T_0^2]$, with $\Omega_0 = 2\pi \times 700 \text{ MHz}$ [58], $T_0 = 0.323$ μs, and $\tau = 1$ μs, we simulate the time evolution of the system by solving the Schrödinger
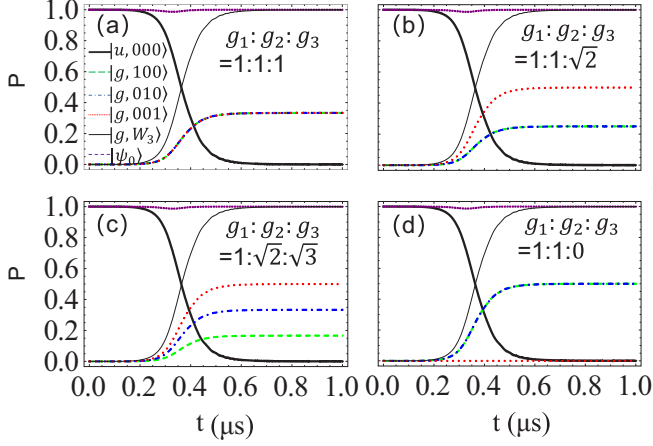
FIG. 2. Adiabatic transfer from $|u, 000\rangle$ to $|g, W_3\rangle$ obtained by numerical simulation. Population of states $|u, 000\rangle$, $|g, 100\rangle$, $|g, 010\rangle$, $|g, 001\rangle$, dark state $|\Psi_0\rangle$, and final state $|g, W_3\rangle$ as a function of time for $\Delta_1 = \Delta_2 = 0$, $\Omega = \Omega_0 \exp[-(t - \tau)^2/T_0^2]$, with $\Omega_0 = 2\pi \times 700$ MHz, $T_0 = 0.323$ μs, and $\tau = 1$ μs. The couplings in panels (a)–(d) are $2g_1/2\pi = 8.64$, $4.32\sqrt{3}$, $8.64\sqrt{2}$, and $8.64\sqrt{3/2}$ MHz, respectively.

equation numerically. As can be seen in Fig. 2, the adiabatic fidelity [59–61] $|\langle \psi(t)|\Psi_0\rangle|^2$ is close to 1 at all time and the fidelity $F(t) = |\langle \psi(t)|g, W_3\rangle|^2$ increases as the pump pulse rises and finally approaches unity when $\Omega \gg g_i$.

Consequently, our proposal is testified by numerical results. Now we study the relation between evolution time and fidelity. Ideally, $F(t)$ finally reaches $\Omega_0^2/(4A^2 + \Omega_0^2)$ at $t = \tau$. Since the highest $\Omega_0/2\pi$ we find in circuit QED experiments ≈ 1 GHz [58] under the RWA, $A/2\pi$ can be some tens of MHz to ensure a high fidelity at the end of the adiabatic evolution, under the adiabatic condition [62–64]

$$\left| \frac{\langle \Psi_\pm(t)|\dot{\Psi}_0(t)\rangle}{E_0 - E_\pm} \right| \ll 1, \quad t \in [0, \tau], \quad (8)$$

which reduces to

$$\frac{4A\dot{\Omega}(t)}{\sqrt{(4A^2 + \Omega(t)^2)\mathcal{N}_\pm}} \ll \left| \Delta_1 \pm \sqrt{4A^2 + \Delta_1^2 + \Omega(t)^2} \right|, \quad (9)$$

according to Eqs. (6) and (7). In most cases, STIRAP works best for $\Delta = 0$ [65], where Eq. (9) becomes

$$\frac{2\sqrt{2}A\dot{\Omega}(t)}{4A^2 + \Omega(t)^2} \ll \sqrt{4A^2 + \Omega(t)^2}. \quad (10)$$

Then we integrate Eq. (10) in the time interval $[0, \tau]$ to obtain a "global" adiabatic condition [65]. If we define $\tan \theta = \Omega/2A$, then $|\Psi_0\rangle = \cos \theta |u, 000\rangle - \sin \theta |g, W_3\rangle$ and $\frac{2A\dot{\Omega}}{4A^2 + \Omega^2} = \dot{\theta}$. Therefore the "global" adiabatic condition reads

$$\int_0^\tau \sqrt{4A^2 + \Omega(t)^2}dt \gg \int_0^{\pi/2} \sqrt{2}d\theta = \pi/\sqrt{2}, \quad (11)$$

coinciding with the results for a similar system in Refs. [65,66]. Here $\tau = 1$ μs and $F(\tau) \approx 99.968\%$. Selecting specific couplings, we can generate a prototype W state $\frac{1}{\sqrt{3}}(|100\rangle + |010\rangle + |001\rangle)$, shown in Fig. 2(a), a perfect W state $\frac{1}{2}(|100\rangle + |010\rangle + \sqrt{2}|001\rangle)$ in Fig. 2(b), a common one
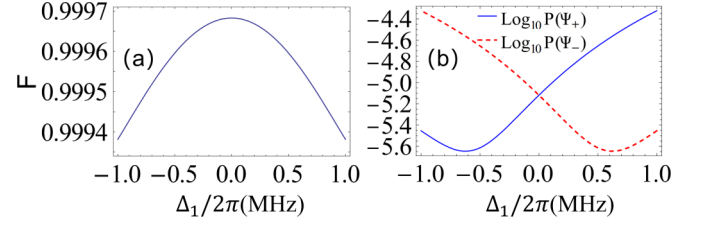
FIG. 3. Effects of detuning on W-state generation shown in Fig. 2(a). (a) The effect of detuning Δ_1 on generation fidelity F of $|W_3\rangle$. (b) The relation between detuning Δ_1 and the population of two bright eigenstates $\Psi_\pm$ at the end of adiabatic evolution.

$\frac{1}{\sqrt{6}}(|100\rangle + 1/\sqrt{2}|010\rangle + \sqrt{3}|001\rangle)$ in Fig. 2(c), and a Bell state $\frac{1}{\sqrt{2}}(|10\rangle + |01\rangle)$ in Fig. 2(d). The fidelities $F(t)$ are equal anytime in these cases. We will explain it and show its usage in the last section. Taking the case shown in Fig. 2(a) for example, we find $F(\tau)$ is not sensitive to detunings, whose maximum is reached at $\Delta_1 = \Delta_2 = 0$. Meanwhile, populations of bright states $\Psi_\pm$ is smaller than 10^{-4} at $t = \tau$ for $\Delta_1/2\pi = \Delta_2/2\pi$ ranging from -1 to 1 MHz, as shown in Fig. 3.

In practice, it is unavoidable to consider the effects of environment, which are studied here with the Lindblad master equation [67–72]:

$$\frac{d\rho}{dt} = -i[H, \rho] + \sum_{i=1}^{N+3} \frac{1}{2}(2L_i\rho L_i^\dagger - L_i^\dagger L_i\rho - \rho L_i^\dagger L_i), \quad (12)$$

where $L_1 = \sqrt{\kappa_1}|g, 000\rangle\langle g, 100|$, $L_2 = \sqrt{\kappa_2}|g, 000\rangle\langle g, 010|$, $L_3 = \sqrt{\kappa_3}|g, 000\rangle\langle g, 001|$, $L_{N+1} = \sqrt{\gamma_e/2}(|u, 000\rangle\langle e, 000| + |g, 000\rangle\langle e, 000|)$, $L_{N+2} = \sqrt{2\gamma_{\varphi e}}|e, 000\rangle\langle e, 000|$, $L_{N+3} = \sqrt{2\gamma_{\varphi u}}|u, 000\rangle\langle u, 000|$, and N is the resonator mode number which equals three here. The qutrit excited state $|e\rangle$ possesses a lifetime $(\gamma_e)^{-1}$, where we have assumed its decay rates to $|u\rangle$ and $|g\rangle$ are equal, and pure dephasing times $(\gamma_{\varphi e})^{-1}$ for $|e\rangle$, $(\gamma_{\varphi u})^{-1}$ for $|u\rangle$. The lifetime of the each resonator κ_i^{-1} is assumed to be equal to κ^{-1}. The system parameters are chosen as in Fig. 2(a), and we first consider the dephasing effects. As shown in Fig. 4(a), the fidelity is not sensitive to $\gamma_{\varphi e}$, and the quantum computation target 99.9% [73] is reached when $\gamma_{\varphi e} < 0.22$ (μs^{-1}). But when we take into account the dephasing of $|u, 000\rangle$ as in Ref. [73], we find a sharp decrease of F even for a small $\gamma_{\varphi u}$, as shown by the solid blue line in Fig. 4(b). $F > 99.9\%$ for $\gamma_{\varphi u} < 0.008$ (μs^{-1}), which is demanding but can be realized in experiment [74,75]. The damping of the qutrit has no significant effects on F, as shown in Fig. 4(c). However, F is sensitive to the resonator dissipation, as shown in Fig. 4(d). $F > 99.9\%$ when $\kappa < 0.001$ (μs^{-1}), which can be realized in experiment [76,77]. Finally, we combine all above factors, and choose $\gamma_e/2 = \gamma_{\varphi e} = 0.01$ (μs^{-1}), $\kappa = 10^{-4}$ (μs^{-1}). The fidelity as a function of $\gamma_{\varphi u}$ is depicted as the red dashed line in Fig. 4(b), which almost overlaps with the blue solid line. If we choose $\gamma_e/2 = \gamma_{\varphi e} = 1$ (μs^{-1}), $\kappa = 0.01$ (μs^{-1}), the fidelity will decrease about 1%, as the dot-dashed line shown in Fig. 4(b). We have also considered the dephasing of $|g\rangle$, and the result is very similar to that of $|u\rangle$, so we do not show it here.
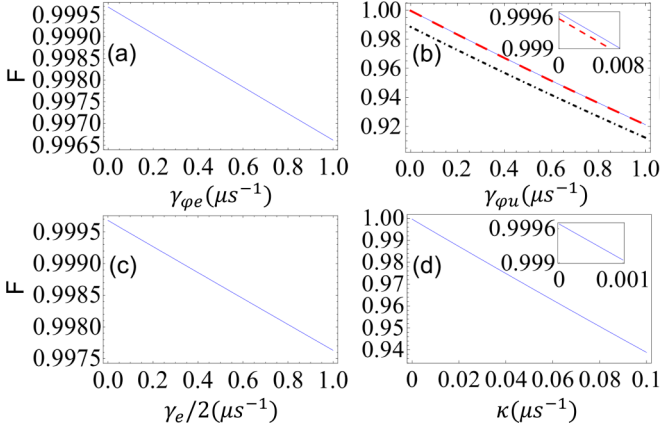
FIG. 4. The environment effects on the fidelity F of $|W_3\rangle$ generated in Fig. 2(a). (a) F as a function of dephasing rate of $|e, 000\rangle$, where $\gamma_e = \gamma_{\varphi u} = \kappa = 0$. (b) F as a function of dephasing rate of $|u, 000\rangle$. $\gamma_e = \gamma_{\varphi e} = \kappa = 0$ for the solid line. $\gamma_e/2 = \gamma_{\varphi e} = 0.01 \, (\mu s^{-1})$, $\kappa = 10^{-4} \, (\mu s^{-1})$ for the red dashed line. $\gamma_e/2 = \gamma_{\varphi e} = 1 \, (\mu s^{-1})$, $\kappa = 0.01 \, (\mu s^{-1})$ for the dot-dashed line. (c) Fidelity as a function of $\gamma_e/2$, where $\kappa = \gamma_{\varphi u} = \gamma_{\varphi e} = 0$. (d) F as a function of resonator dissipation κ, where $\gamma_e = \gamma_{\varphi u} = \gamma_{\varphi e} = 0$.

III. EMISSION OF THE SINGLE-PHOTON THREE-MODE W STATES

Our scheme to emit the single-photon W state is shown in Fig. 5. Each CWR is coupled to a transmission line (TL) through a variable coupler C, so that its dissipation rate κ into the TL is tunable [78]. We are able to generate a single-photon W state inside CWRs when C is turned off, as discussed above. If we turn on each C with the same κ, then the W state is released into the TLs, overcoming its disadvantage of uneasy to be detected [26]. First, we give an intuitive explanation. Any initial superposition state of the form

$$g_1|g, 100\rangle + g_2|g, 010\rangle + g_3|g, 001\rangle \qquad (13)$$

will be finally transformed to

$$|g, 000\rangle \otimes (g_1|100\rangle_{out} + g_2|010\rangle_{out} + g_3|001\rangle_{out}) \qquad (14)$$
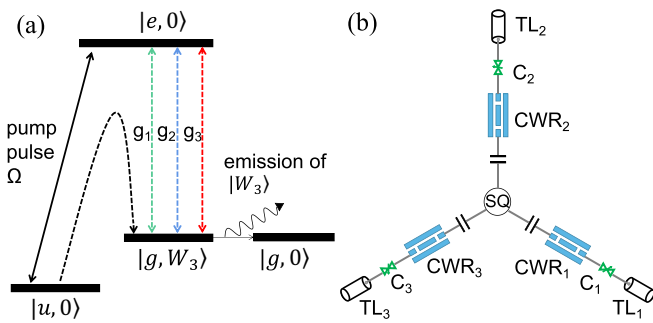
FIG. 5. The scheme to emit the single-photon three-mode W state $|W_3\rangle$. (a) Relevant energy levels and transitions. (b) Setup: we add a variable coupler [78] to control the dissipation rate of each CWR into the corresponding transmission line (TL).

through leakage resonators with the same dissipation rate, where $|100\rangle_{out}$, $|010\rangle_{out}$, $|001\rangle_{out}$ denote there is one photon in the output channel of the first, second and third resonators respectively, considering $a_{iout}(t) = \sqrt{\kappa}a_i(t)$, $i = 1, 2, 3$ [58,79] in the Heisenberg picture. On the contrary to the last section, a large κ is required here to accelerate the emission of the W state. κ includes an intrinsic part and an external part caused by the coupler C. The former is neglected here because it can be chosen as $1/1000$ of the later which reaches 0.2 (ns^{-1}) in experiment [78].

Now we give a more rigorous analysis from the Lindblad master equation (12). Supposing the system is in an incoherent superposition of pure states $\rho = \sum p_m|\psi_m\rangle\langle\psi_m|$ with

$$|\psi_m\rangle = c_{um}|u, 000\rangle + c_{em}|e, 000\rangle + c_{1m}|g, 100\rangle$$
$$+ c_{2m}|g010\rangle + c_{3m}|g001\rangle + c_{gm}|g000\rangle, \qquad (15)$$

where p_m is the probability of $|\psi_m\rangle$ and m identifies one possible pure state. Since $c_{um} = 1$ initially and $\kappa_i = \kappa$, we find $c_{1m} : c_{2m} : c_{3m} = g_1 : g_2 : g_3$ is a solution to

$$\frac{d(c_{1m}c_{1m}^*)}{dt} = -ig_1(c_{em}c_{1m}^* - c_{em}^*c_{1m}) - \kappa c_{1m}c_{1m}^*, \quad (16)$$

$$\frac{d(c_{2m}c_{2m}^*)}{dt} = -ig_2(c_{em}c_{2m}^* - c_{em}^*c_{2m}) - \kappa c_{2m}c_{2m}^*, \quad (17)$$

$$\frac{d(c_{3m}c_{3m}^*)}{dt} = -ig_3(c_{em}c_{3m}^* - c_{em}^*c_{3m}) - \kappa c_{3m}c_{3m}^*. \quad (18)$$

Meanwhile, $\rho_{ij} = \sum_m p_m c_{im} c_{jm}^*$, so that the master equation (12) can be satisfied. Therefore, the emission rate of each mode $\kappa Tr(\rho a_i^\dagger a_i)$ and its probability $\kappa \int \text{Tr}(\rho a_i^\dagger a_i)dt$ will be proportional to g_i^2, and a desired $|W_3\rangle = \frac{1}{A}(g_1|100\rangle_{out} + g_2|010\rangle_{out} + g_3|001\rangle_{out})$ could be created in the output channels considering $a_{iout}(t) = \sqrt{\kappa}a_i(t)$ and the whole system will end up with Eq. (14). Choosing the pump pulse Ω and coupling g_i as shown in Figs. 6(a) and 6(b), the population transfer under dissipation are shown in Figs. 6(c) and 6(d). The single-photon W state is created at the rising edge of the pump pulse and emitted through the leakage resonators. Here we choose a sawtooth-shaped Rabi frequency as in Refs. [57,80], which has merits [57] and gives a higher emission rate than the typical Gaussian type in our numerical simulation, while the latter has higher fidelity in generating W states inside resonators, since they are two different processes. In the latter case, the system has to strictly follow the adiabatic path under condition Eq. (8), so the adiabatic speed is limited by the gap $|\Delta_1 \pm [4A^2 + \Omega(t)^2 + \Delta_1^2]^{1/2}|/2$. $\Omega(t)$ increases from about zero to much larger than $2A$. The gap is small in early times, so $\langle\Psi_\pm|\dot\Psi_0\rangle \sim \dot\Omega(t)$ must also be small there to satisfy Eq. (8). In this sense, a Gaussian pulse is better than a linear one. But in the fast emission process where κ is large, the system will not always stay in $|\Psi_0(t)\rangle$, because the coherent superposition between $|u, 000\rangle$ and $|g, W_3\rangle$ will get lost due to the release of $|W_3\rangle$. Therefore $\Psi_\pm$ are also populated, which contains a contribution from $|e, 000\rangle$ [55]. However, this will not hinder the emission of $|W_3\rangle$ since the damping and dephasing rate of $|e\rangle$ can be very small. Its population will be transferred to $|g, W_3\rangle$, and $|W_3\rangle$ will still be emitted through resonator dissipation. Now the key point is to quickly transfer $|u, 000\rangle$ to $|e, 000\rangle$ and then to $|g, W_3\rangle$. Starting with the same $\Omega(0) \approx 0$, a linear shape pulse will increase faster than the Gaussian
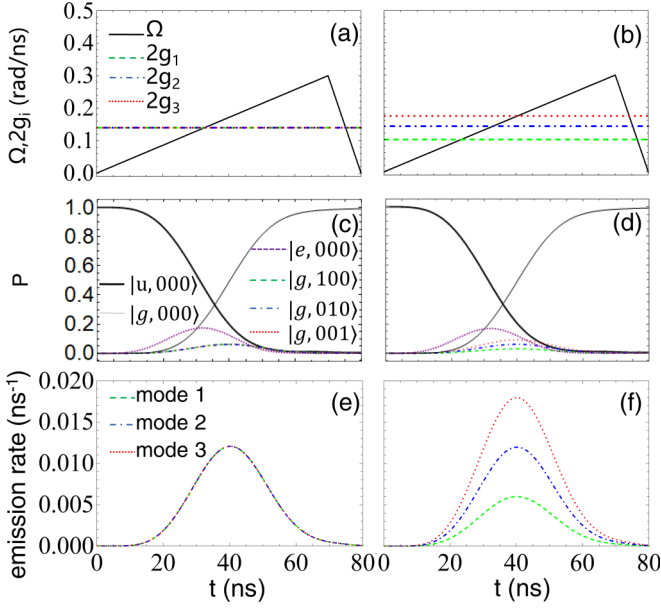
FIG. 6. Simulation of the W-state emission by solving the Lindblad master equation (12) numerically. $|W_3\rangle = \frac{1}{\sqrt{3}}(|100\rangle + |010\rangle + |001\rangle)$ in the left panel and $\frac{1}{\sqrt{6}}(|100\rangle + \sqrt{2}|010\rangle + \sqrt{3}|001\rangle)$ in the right panel. $\Delta_1 = \Delta_2 = 0.02$ rad/ns. $\gamma_e/2 = 2\gamma_{\varphi e} = 0.04$ (μs^{-1}). $\kappa_i = \kappa = 0.2$ ns^{-1}. (a), (b) Pump pulses and coupling strength between qutrit and each resonator. (c), (d) Population of states $|u, 000\rangle$, $|g, 100\rangle$, $|g, 010\rangle$, $|g, 001\rangle$, $|g, 000\rangle$ inside resonators. (e), (f) Emission rate of each mode into the corresponding transmission line.

shape and the transfer will be faster. However, $\Omega(t)$ cannot be too large, which will make the oscillation between $|u\rangle$ and $|e\rangle$ so fast that the emitted photon waveform would become nonsymmetric and multipeaked, not good for its reabsorption by quantum nodes [58]. To quantify the symmetry of the photon waveform, we define

$$s = \frac{\int_0^{2T_0} \langle a_{iout}^\dagger(t) a_{iout}(t)\rangle \langle a_{iout}^\dagger(2T_0 - t) a_{iout}(2T_0 - t)\rangle dt}{\int_0^{2T_0} \langle a_{iout}^\dagger(t) a_{iout}(t)\rangle^2 dt},$$
(19)

similar to [58], where T_0 is at the peak of the waveform and s is actually independent of i here. Choosing $\gamma_e/2 = 2\gamma_{\varphi e} = 0.04$ (μs^{-1}) [77], $\kappa_i = \kappa = 0.2$ (ns^{-1}) [78], $\Omega_{max} = 0.3$ rad/ns [81], which are within the reach of experiment, the W states can be emitted in 80 ns with probability $P = 99.12\%$ and $s = 0.999$, as shown in Fig. 6(e), while $P = 99.13\%$ and $s = 0.9987$ in Fig. 6(f). We do not take into account the dephasing of $|u\rangle$ or $|g\rangle$ here and hereafter, because unlike the case of generating W states inside resonators, it has little effect on emission probabilities even for $2\gamma_{\varphi u,g} = 0.04$ (μs^{-1}). The emission rate and probability of the ith resonator are proportional to g_i^2 for $\kappa_i = \kappa$, which means that the output single-photon state could still possesses the structure of $g_1|100\rangle + g_2|010\rangle + g_3|001\rangle$, an easily tunable W state, as shown in Figs. 6(e) and 6(f). Similar to the generation of W_3 inside resonators, the emission probability P is not sensitive to detunings, but $\Delta_1 = 0$ is no longer always most efficient. $P = 99.12\%$ when $\Delta_1 = 0.02$ rad/ns and $P = 99.10\%$ for $\Delta_1 = 0$.
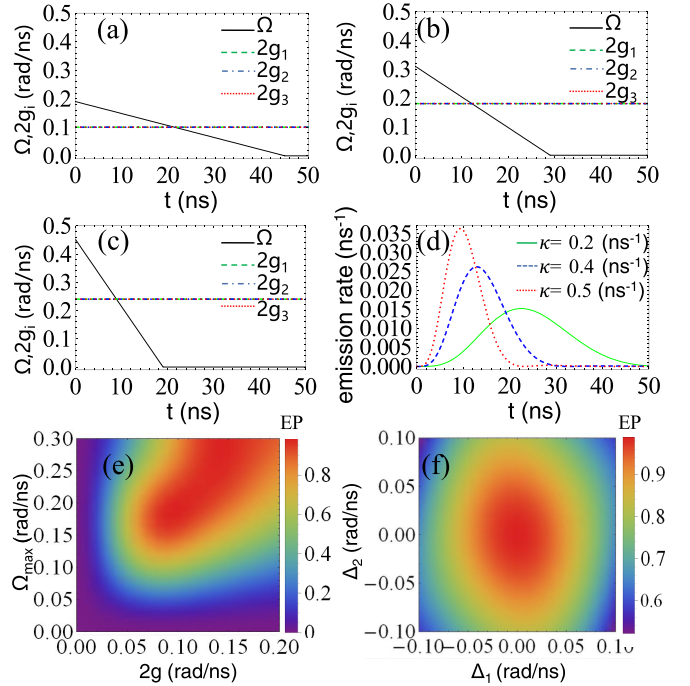
FIG. 7. Fast emission of the W state using certain parameters. $\gamma_e/2 = 2\gamma_{\varphi e} = 0.04$ (μs^{-1}). (a)–(c) g_i and Ω used for $\kappa = 0.2$ (ns^{-1}), 0.4 (ns^{-1}), 0.5 (ns^{-1}) in numerical simulation, respectively. (d) The corresponding photon wave packets of each mode, which are overlapped since the couplings and emission rates are equal. $\Delta_1 = \Delta_2 = 0$. (e) Emission probabilities (EP) in 50 ns against $2g$ and Ω_{max}, for $\kappa = 0.2$ (ns^{-1}), $\Delta_1 = \Delta_2 = 0$. (f) EP in 50 ns against Δ_1 and Δ_2, for $\kappa = 0.2$ (ns^{-1}), Ω and g chosen as in panels (a).

The emission rate and probability depend on g_i, κ, γ, $\gamma_{\varphi e}$, Δ_1, Δ_2, and Ω, and we shall explore a combination of parameters available for fast rate, high probability, and symmetric waveform [58]. For simplicity, we consider $g_1 = g_2 = g_3 = g$, so that the photon emission rate for three resonators are the same and their wave packets are overlapped. The maximum κ we found in experiment is 0.2 (ns^{-1}) [78], but in principle, it could be larger in the bad-cavity limit [77,82,83]. So we consider $\kappa = 0.2$ (ns^{-1}), 0.4 (ns^{-1}), 0.5 (ns^{-1}), and choose different combinations of Ω and g for the fast emission of the W state, which are shown in Figs. 7(a)–7(c), respectively. The corresponding emission probabilities of the prototype W state reach 98.9% in 50 ns with $s = 0.989$, 99.5% in 30 ns with $s = 0.983$, and 98.9% in 20 ns with $s = 0.99$, respectively, as shown in Fig. 7(d), comparable to the recently reported fastest two-qubit gate (30–45 ns) [54]. Here $\gamma_e/2 = 2\gamma_{\varphi e} = 0.04$ (μs^{-1}) [77], and $\Delta_1 = \Delta_2 = 0$.

These parameters are chosen based on analyses and numerical experiments. First, as can be seen from Figs. 7(a)–7(d), a combination of larger κ, g, and Ω will make the photon wave packet sharper and shifted towards earlier time. The system is initially in $|u, 0\rangle$, so a large Ω at $t = 0$ will transfer the population to $|e, 0\rangle$ quickly. Meanwhile, a proper combination of g and κ will quickly transfer the population of $|e, 0\rangle$ to $|g, W_3\rangle$ and release the photon. We find a linear decreasing shape of $\Omega(t)$ will make the photon wave packet more symmetric in time and centered at one peak. Because a large $\Omega(t)$ will make

a fast oscillation between $|u\rangle$ and $|e\rangle$, such that the photon waveform will be multipeaked. Here we limit the total evolution time $T = 50$ ns, and $\Omega(t) = \Omega_{max}(1 - t/t_f)\Theta(t_f - t)$. Taking $\kappa = 0.2$ (ns^{-1}) for example, we choose $t_f = 45$ ns, and search for the best combination of g and Ω_{max} to give the maximum emission probability numerically, as shown in Fig. 7(e). The best choice ($2g = 0.1$ rad/ns, $\Omega_{max} = 0.19$ rad/ns) is depicted in Fig. 7(a). Second, damping γ_e and dephasing $\gamma_{\varphi e}$ will reduce the emission probability, so we choose very small γ_e and $\gamma_{\varphi e}$ available for superconducting qubits [77]. Last, for the case shown in Fig. 7(a) with $\kappa = 0.2$ (ns^{-1}), we change parameters Δ_1 and Δ_2 to find the maximum emission probability reached at the resonance condition $\Delta_1 = \Delta_2 = 0$, shown in Fig. 7(f).

IV. GENERATION AND EMISSION OF ARBITRARY SINGLE-PHOTON MULTIMODE W STATES WITH THE SAME FIDELITY AND TIME

Here we extend our scheme to generate and emit arbitrary single-photon multimode W states $|W_N\rangle = \frac{1}{A}\sum_{i=1}^{N} A_i |0_1 0_2 \cdots 1_i 0_{i+1} \cdots 0_N\rangle$. The system is in principle the same as Fig. 5, just with resonator number added to N.

The Hamiltonian of this system in the one-photon manifold under the RWA becomes

$$
\begin{aligned}
H = &\sum_{j=u,e,g} E_j |j, 00\cdots 0\rangle\langle j, 00\cdots 0| \\
&+ (E_g + \omega)\Bigg(\sum_{i=1}^{N} |g, 0_1 0_2 \cdots 1_i 0_{i+1} \cdots 0_N\rangle \\
&\otimes \langle g, 0_1 0_2 \cdots 1_i 0_{i+1} \cdots 0_N| \Bigg) \\
&+ \Bigg(\frac{1}{2}\Omega e^{-i\omega_p t} |e, 00\cdots 0\rangle\langle u, 00\cdots 0| \\
&+ \sum_{i=1}^{N} g_i |g, 0_1 0_2 \cdots 1_i 0_{i+1} \cdots 0_N\rangle\langle e, 00\cdots 0| + \text{H.c.} \Bigg).
\end{aligned}
$$
(20)

First we consider the generation of W states inside resonators. Supposing all dissipations are negligible, and the system is in state $|\psi\rangle = c_u |u, 000\rangle + c_e |e, 000\rangle + \sum_{i=1}^{N} c_i |0_1 0_2 \cdots 1_i 0_{i+1} \cdots 0_N\rangle$. Similar to the three-mode case, we solve the eigenenergy equation in the interaction picture and find N degenerate dark states $\{2g_1 |u, 00\cdots 0\rangle - \Omega|g, 10\cdots 0\rangle, \quad 2g_2 |u, 00\cdots 0\rangle - \Omega|g, 01\cdots 0\rangle, \ldots, 2g_N |u, 000\rangle - \Omega|g, 00\cdots 1\rangle\}$ with $E = 0$. On the other hand, according to the Schrödinger equation $\dot{c}_i = ig_i c_e$ with initial condition $c_u = 1$, we find $c_i(t)/c_j(t) = g_i/g_j$. Hence the dark state in this specific case reads:

$$
|\Psi_0\rangle = \frac{1}{\sqrt{4A^2 + \Omega^2}}[2A|u, 000\rangle - \Omega|g, W_N\rangle], \quad (21)
$$

where $|W_N\rangle = \frac{1}{A}\sum_{i=1}^{N} g_i |0_1 0_2 \cdots 1_i 0_{i+1} \cdots 0_N\rangle$, and $A = (\sum_{i=1}^{N} g_i^2)^{1/2}$. To create an arbitrary $|W_N\rangle$, we need to set g_i

and N as required and then turn on the pump pulse which rises slowly to adiabatically transfer $|u, 00\cdots\rangle$ to the target state. We shall explore a combination of parameters which gives high fidelity and speed available for all mode numbers, as we have done for the three-mode case.

The ideal fidelity $F = |\langle g, W_N |\Psi_0\rangle|^2 = \Omega^2/(4A^2 + \Omega^2)$, meanwhile, the energy gap limiting the adiabatic speed is $|\Delta_1 \pm (4A^2 + \Omega^2 + \Delta_1^2)^{1/2}|/2$, so intuitively, if $A = (\sum_{i=1}^{N} g_i^2)^{1/2}$ and other parameters are fixed for different N, the fidelity and evolution time will both be the same. We give a more rigorous proof using the Schrödinger equation

$$
\frac{dc_u}{dt} = -\frac{i}{2}\Omega c_e,
$$

$$
\frac{dc_e}{dt} = -\frac{i}{2}\left(\Omega c_u + 2\Delta_1 c_e + \sum_{i=1}^{N} 2g_i c_i \right),
$$

$$
\frac{dc_i}{dt} = -ig_i c_e.
$$

It is easy to find if

$$
\sum_{i'=1}^{N'} g_{i'}'^2 = \sum_{i=1}^{N} g_i^2 \tag{22}
$$

for mode number N', with other parameters fixed, then

$$
c_e'(t) = c_e(t), \tag{23}
$$

$$
c_u'(t) = c_u(t), \tag{24}
$$

$$
c_i(t)/c_j(t) = g_i/g_j, \tag{25}
$$

$$
c_{i'}'(t)/c_i(t) = g_{i'}'/g_i, \tag{26}
$$

are solutions of the Schrödinger equation for mode numbers N and N', where $c_e'(t)$, $c_u'(t)$, and $c_{i'}'(t)$ are corresponding wave functions for N' case. Therefore, the fidelity to obtain $|W_N\rangle$ and $|W_{N'}'\rangle$ are the same at any time according to Eqs. (22) and (26). Once we find a combination of parameters to generate a W state with high speed and fidelity, we equally find it for arbitrary ones by using Eq. (22) (N' can equal N). And that is why the generation time and fidelity are both the same for different three-mode W states, as shown in Fig. 2. Now we testify it for different mode numbers. For simplicity, we assume all g's ($i = 1, 2, \ldots, M$) equal to g_M for M-mode case. Choosing the same parameters as the three-mode case shown in Fig. 2(a) except for $g_M = \sqrt{3}g_3/\sqrt{M} = g_1/\sqrt{M}$ with M ranging from 1 to 20, as depicted in Fig. 8(c), we find the fidelities are all equal to 99.968% in 1 μs by solving the Schrödinger equation numerically, shown in Fig. 8(a).

Then we consider the emission of $|W_N\rangle$ using the master equation (12) with N extended to arbitrary positive integers. First we assume the system is in an incoherent superposition of pure states $\rho = \sum_m p_m |\psi_m\rangle\langle\psi_m|$ with $|\psi_m\rangle = c_{um}|u, 00\cdots 0\rangle + c_{em}|e, 00\cdots 0\rangle + \sum_{i=1}^{N} c_{im}|g, 00\cdots 1_i 0_{i+1} 0_N\rangle + c_{gm}|g00\cdots 0\rangle$ with $c_{um} = 1$ initially and $\kappa_i = \kappa$. Then, following the same routine as the three-mode case, we can prove the emission rate of each resonator $\kappa\langle a_i^\dagger a_i\rangle$ is proportional to g_i^2, and an adjustable single-photon multimode
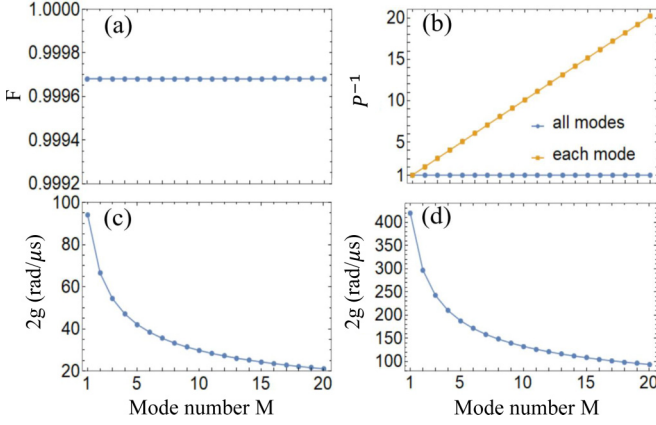
FIG. 8. Fidelities of $|W_M\rangle = \frac{1}{M}\sum_{i=1}^{M}|0_1 0_2 \cdots 1_i 0_{i+1}\cdots 0_M\rangle$ within the same evolution time for different M. (a) Fidelities of generating $|W_M\rangle$ inside resonators in 1 μs, which are all equal to 99.968%, with M ranging from 1 to 20. The parameters for each mode is the same as the three-mode case shown in Fig. 2(a), except for $g_M = \sqrt{3}g_3/\sqrt{M} = g_1/\sqrt{M}$, which is depicted in panel (c). (b) Reciprocal of emission probabilities P^{-1} of $|W_M\rangle$ (all modes and each mode) into transmission lines in 20 ns for different M. The total P equals 98.93% for each M, where P for the ith mode is $\frac{98.93}{M}$%. $\kappa = 0.5$ (ns^{-1}). $\Delta_1 = \Delta_2 = 0$. Ω is chosen as Fig. 5(c), and $\gamma_e/2 = \gamma_{\varphi e} = 0.04$ (μs^{-1}). $g_M = g_1/\sqrt{M}$ with $2g_1 = 420$ rad/μs, as shown in panel (d).

W state could be emitted. In practice, we need to find proper parameters to release the W states with high rate and probability for arbitrary N, as we have done for the three-mode case.

For each $|\psi_m\rangle\langle\psi_m|$, the master equation (12) with subscript "m" neglected reads

$$\frac{d(c_i c_i^*)}{dt} = ig_i(c_e^* c_i - c_e c_i^*) - \kappa c_i c_i^*, \qquad (27)$$

$$\frac{d(c_e c_e^*)}{dt} = -\frac{i}{2}\left[\Omega(c_u c_e^* - c_u^* c_e) + \sum_{i=1}^{N} 2g_i(c_i c_e^* - c_i^* c_e)\right]$$
$$- \gamma_e c_e c_e^*, \qquad (28)$$

$$\frac{d(c_u c_u^*)}{dt} = -\frac{i}{2}\Omega(c_e c_u^* - c_e^* c_u) + \frac{\gamma_e}{2}c_e c_e^*, \qquad (29)$$

$$\frac{d(c_u c_e^*)}{dt} = -\frac{i}{2}\left[\Omega(c_e c_e^* - c_u^* c_u) - \sum_{i=1}^{N} 2g_i c_u c_i^* - 2\Delta_1 c_u c_e^*\right]$$
$$- \left(\frac{\gamma_e}{2} + \gamma_{\varphi e}\right)c_u c_e^*, \qquad (30)$$

$$\frac{d(c_u c_i^*)}{dt} = -\frac{i}{2}[\Omega c_e c_i^* - 2g_i c_u c_e^*] - \frac{\kappa}{2}c_u c_i^*, \qquad (31)$$

$$\frac{d(c_e c_i^*)}{dt} = -\frac{i}{2}\left[\Omega c_u c_i^* + \sum_{j=1}^{N} 2g_j c_j c_i^* + 2\Delta_1 c_e c_i^* - 2g_i c_e c_e^*\right]$$
$$- \left(\gamma_{\varphi e} + \frac{\gamma_e + \kappa}{2}\right)c_e c_i^*, \qquad (32)$$

$$\frac{d(c_i c_j^*)}{dt} = i[g_j c_i c_e^* - g_i c_e c_j^*] - \kappa c_i c_j^*. \qquad (33)$$

We find Eqs. (23)–(26) are still solutions of the above equation set for different mode numbers N and N' under the condition $\sum_{i'=1}^{N'} g_{i'}^2 = \sum_{i=1}^{N} g_i^2$ and with the other parameters fixed. The total emission rates $\kappa \sum_i^N |c_i|^2$ and $\kappa \sum_{i'=1}^{N'} |c_{i'}'|^2$ are equal according to Eqs. (22) and (26). So in this specific case, the total emission rate and probability of $|W_N\rangle$ and $|W_{N'}'\rangle$ will be the same at anytime. For simplicity, we assume all g_i ($i = 1, 2, \ldots, M$) are equal to g_M for the M-mode case in numerical simulation. Then we choose $g_M = g_1/\sqrt{M}$ with $2g_1 = 420$ rad/μs and M ranging from 1 to 20, as shown in Fig. 8(d), while fixing other parameters as in the three-mode case. The total emission rates and emission probabilities P are found to be equal for any mode number M, where the emission probability P for the ith mode is naturally $1/M$ of the total emission probability, which reaches 98.93% in 20 ns, as shown in Fig. 8(b).

V. CONCLUSION

We proposed a unified deterministic scheme of generating and releasing arbitrary single-photon multimode W state on demand with high emission rate, experimental feasibility and symmetric waveform. Essentially, the preparation times do not depend on mode numbers. We have a qutrit coupled to N spatially separated resonators and a pump pulse. Making the system evolve adiabatically along a dark state, we obtain arbitrary W states inside resonators. The first merit of our scheme is the coefficient for the ith basis $|0_1 0_2 \cdots 1_i 0_{i+1} \cdots 0_N\rangle$ of this W state is proportional to the coupling strength of the ith mode g_i, so we can obtain arbitrary W state by tuning this coupling. Second, we can release such W states with symmetric temporal profile into transmission lines on demand by adding a variable coupler to modulate the dissipation rate of the resonators. The emission probabilities reach 98.9% in 20–50 ns, depending on parameters, comparable to the fastest two-qubit gate recently reported. Third, we only need to vary the pump-laser pulse during the time evolution process, which is easier to control than the qutrit. Last, the generation (or emission) time and fidelity (or probability) can both be the same for N-mode and N'-mode cases (N, N' are arbitrary natural numbers), by choosing $\sum_{i'=1}^{N'} g_{i'}^2 = \sum_{i=1}^{N} g_i^2$ and other parameters fixed. Therefore, once we find a proper combination of parameters for the fast generation (emission) of one W state, we equally find it for arbitrary ones. It could be interesting to consider its experimental realization in circuit QED or related systems.

[1] C. H. Bennett and S. J. Wiesner, Communication via One- and Two-Particle Operators on Einstein-Podolsky-Rosen States, Phys. Rev. Lett. **69**, 2881 (1992).

[2] C. H. Bennett, G. Brassard, C. Crépeau, R. Jozsa, A. Peres, and W. K. Wootters, Teleporting an Unknown Quantum State via Dual Classical and Einstein-Podolsky-Rosen Channels, Phys. Rev. Lett. **70**, 1895 (1993).

[3] A. K. Ekert, Quantum Cryptography Based on Bell's Theorem, Phys. Rev. Lett. **67**, 661 (1991).

[4] L. K. Grover, Quantum Mechanics Helps in Searching for a Needle in a Haystack, Phys. Rev. Lett. **79**, 325 (1997).

[5] A. Einstein, B. Podolsky, and N. Rosen, Can Quantum-Mechanical Description of Physical Reality Be Considered Complete, Phys. Rev. **47**, 777 (1935).

[6] W. Dür, G. Vidal and J. I. Cirac, Three qubits can be entangled in two inequivalent ways, Phys. Rev. A **62**, 062314 (2000).

[7] M. Kafatos, *Bell's Theorem, Quantum Theory and Conceptions of the Universe* (George Mason University Press, Fairfax, Virginia, USA, 1989).

[8] C. P. Yang, Q. P. Su, and S. Han, Generation of Greenberger-Horne-Zeilinger entangled states of photons in multiple cavities via a superconducting qutrit or an atom through resonant interaction, Phys. Rev. A **86**, 022329 (2012).

[9] Y. Zhang, T. Liu, J. L. Zhao, Y. Yu, and C. P. Yang, Generation of hybrid Greenberger-Horne-Zeilinger entangled states of particlelike and wavelike optical qubits in circuit QED, Phys. Rev. A **101**, 062334 (2020).

[10] Z.-H. Liu, J. Zhou, H.-X. Meng, M. Yang, Q. Li, Y. Meng, H.-Y. Su, J.-L. Chen, K. Sun, J.-S. Xu, C.-F. Li, and G.-C. Guo, Experimental test of the Greenberger-Horne-Zeilinger-type paradoxes in and beyond graph states, npj Quantum Inf. **7**, 66 (2021).

[11] F. Ozaydin, S. N. Bugu, C. Yesilyurt, A. A. Altintas, M. Tame, and Ş. K. Özdemir, Fusing multiple W states simultaneously with a Fredkin gate, Phys. Rev. A **89**, 042311 (2014).

[12] A. Cabello, Bell's theorem with and without inequalities for the three-qubit Greenberger-Horne-Zeilinger and W states, Phys. Rev. A **65**, 032108 (2002).

[13] A. A. Gangat, I. P. McCulloch, and G. J. Milburn, Deterministic Many-Resonator W Entanglement of Nearly Arbitrary Microwave States via Attractive Bose-Hubbard Simulation, Phys. Rev. X **3**, 031009 (2013).

[14] A. Sharma and A. A. Tulapurkar, Generation of *n*-qubit W states using spin torque, Phys. Rev. A **101**, 062330 (2020).

[15] M. Menotti, L. Maccone, J. E. Sipe, and M. Liscidini, Generation of energy-entangled W states via parametric fluorescence in integrated devices, Phys. Rev. A **94**, 013845 (2016).

[16] B. Fang, M. Menotti, M. Liscidini, J. E. Sipe, and V. O. Lorenz, Three-Photon Discrete-Energy-Entangled W State in an Optical Fiber, Phys. Rev. Lett. **123**, 070508 (2019).

[17] J. Heo, C. Hong, S. G. Choi, and J. P. Hong, Scheme for generation of three-photon entangled W state assisted by cross-Kerr nonlinearity and quantum dot, Sci. Rep. **9**, 10151 (2019).

[18] M. Eibl, N. Kiesel, M. Bourennane, C. Kurtsiefer, and H. Weinfurter, Experimental Realization of a Three-Qubit Entangled W State, Phys. Rev. Lett. **92**, 077901 (2004).

[19] X. B. Zou, K. Pahlke, and W. Mathis, Generation of an entangled four-photon W state, Phys. Rev. A **66**, 044302 (2002).

[20] L. Dong, J.-X. Wang, Q.-Y. Li, H.-Z. Shen, H.-K. Dong, X.-M. Xiu, Y.-J. Gao, and C. H. Oh, Nearly deterministic preparation

of the perfect W state with weak cross-Kerr nonlinearities, Phys. Rev. A **93**, 012308 (2016).

[21] Y. S. Kim, Y. W. Cho, H. T. Lim, and S. W. Han, Efficient linear optical generation of a multipartite W state via a quantum eraser, Phys. Rev. A **101**, 022337 (2020).

[22] J. Peng, J. C. Zheng, J. Yu, P. H. Tang, G. A. Barrios, J. X. Zhong, E. Solano, F. Albarrán-Arriagada, and L. Lamata, One-Photon Solutions to the Multiqubit Multimode Quantum Rabi Model for Fast W-State Generation, Phys. Rev. Lett. **127**, 043604 (2021).

[23] C. L. Zhang and W. W. Liu, Generation of W state by combining adiabatic passage and quantum Zeno techniques, Indian J. Phys. **93**, 67 (2018).

[24] G. P. Guo, C. F. Li, J. Li, and G. C. Guo, Scheme for the preparation of multiparticle entanglement in cavity QED, Phys. Rev. A **65**, 042102 (2002).

[25] Z. J. Deng, M. Feng, and K. L. Gao, Simple scheme for generating an *n*-qubit W state in cavity QED, Phys. Rev. A **73**, 014302 (2006).

[26] G. C. Guo and Y. S. Zhang, Scheme for preparation of the W state via cavity quantum electrodynamics, Phys. Rev. A **65**, 054302 (2002).

[27] X. Wei and M. F. Chen, Generation of *N*-qubit W state in *N* separated resonators via resonant interaction, Int. J. Theor. Phys. **54**, 812 (2015).

[28] Y. H. Kang, Y. H. Chen, Z. C. Shi, J. Song, and Y. Xia, Fast preparation of W states with superconducting quantum interference devices by using dressed states, Phys. Rev. A **94**, 052311 (2016).

[29] Y. H. Kang, Y. H. Chen, Q. C. Wu, B. H. Huang, J. Song, and Y. Xia, Fast generation of W states of superconducting qubits with multiple Schrödinger dynamics, Sci. Rep. **6**, 36737 (2016).

[30] V. M. Stojanović, Bare-Excitation Ground State of a Spinless-Fermion–Boson Model and W-State Engineering in an Array of Superconducting Qubits and Resonators, Phys. Rev. Lett. **124**, 190504 (2020).

[31] V. M. Stojanović, Scalable W-type entanglement resource in neutral-atom arrays with Rydberg-dressed resonant dipole-dipole interaction, Phys. Rev. A **103**, 022410 (2021).

[32] F. Ozaydin, C. Yesilyurt, S. N. Bugu, and M. Koashi, Deterministic preparation of W states via spin-photon interactions, Phys. Rev. A **103**, 052421 (2021).

[33] D. C. Cole, J. J. Wu, S. D. Erickson, P.-Y. Hou, A. C. Wilson, D. Leibfried, and F. Reiter, Dissipative preparation of W states in trapped ion systems, New J. Phys. **23**, 073001 (2021).

[34] T. Haase, G. Alber, and V. M. Stojanovic, Dynamical generation of chiral W and Greenberger-Horne-Zeilinger states in laser-controlled Rydberg-atom trimers, arXiv:2111.09718.

[35] D. Gottesman, T. Jennewein, and S. Croke, Longer-Baseline Telescopes Using Quantum Repeaters, Phys. Rev. Lett. **109**, 070503 (2012).

[36] S. Guha and J. H. Shapiro, Reading boundless error-free bits using a single photon, Phys. Rev. A **87**, 062306 (2013).

[37] S. B. Papp, K. S. Choi, H. Deng, P. Lougovski, S. J. Van Enk, and H. J. Kimble, Characterization of multipartite entanglement for one photon shared among four optical modes, Science **324**, 764 (2009).

[38] K. S. Choi, A. Goban, S. B. Papp, S. J. van Enk, and H. J. Kimble, Entanglement of spin waves among four quantum memories, Nature (London) **468**, 412 (2010).

[39] K. Li, D. L. Zheng, W. Q. Xu, H. B. Mao, and J. Q. Wang, *W* states fusion via polarization-dependent beam splitter, Quantum Inf. Process. **19**, 412 (2020).

[40] V. N. Gorbachev, A. I. Trubilko, A. A. Rodichkina, and A. Zhiliba, Can the states of the *W*-class be suitable for teleportation, Phys. Lett. A **314**, 267 (2003).

[41] P. Agrawal and A. Pati, Perfect teleportation and superdense coding with *W* states, Phys. Rev. A **74**, 062320 (2006).

[42] L. Z. Li and D. W. Qiu, The states of *W*-class as shared resources for perfect teleportation and superdense coding, J. Phys. A: Math. Theor. **40**, 10871 (2007).

[43] Y. B. Sheng, L. Zhou, and S. M. Zhao, Efficient two-step entanglement concentration for arbitrary *W* states, Phys. Rev. A **85**, 042302 (2012).

[44] L. Zhou, Y. B. Sheng, W. W. Cheng, L. Y. Gong, and S. M. Zhao, Efficient entanglement concentration for arbitrary single-photon multimode *W* state, J. Opt. Soc. Am. B **30**, 71 (2013).

[45] C. P. Yang, Q. P. Su, S. B. Zheng and S. Han, Generating entanglement between microwave photons and qubits in multiple cavities coupled by a superconducting qutrit, Phys. Rev. A **87**, 022320 (2013).

[46] X. L. Zhang, K. L. Gao, and M. Feng, Preparation of cluster states and *W* states with superconducting quantum-interference-device qubits in cavity QED, Phys. Rev. A **74**, 024303 (2006).

[47] Z. J. Deng, K. L. Gao, and M. Feng, Generation of *N*-qubit *W* states with rf SQUID qubits by adiabatic passage, Phys. Rev. A **74**, 064303 (2006).

[48] X. J. Lu, M. Li, Z. Y. Zhao, C. L. Zhang, H. P. Han, Z. B. Feng, and Y. Q. Zhou, Nonleaky and accelerated population transfer in a transmon qutrit, Phys. Rev. A **96**, 023843 (2017).

[49] Q. P. Su, C. P. Yang, and S. B. Zheng, Fast and simple scheme for generating NOON states of photons in circuit QED, Sci. Rep. **4**, 3898 (2015).

[50] Y. H. Liu, D. Lan, X. Tan, J. Zhao, P. Zhao, M. Li, K. Zhang, K. Dai, Z. Li, Q. Liu, S. Huang, G. Xue, P. Xu, H. Yu, S.-L. Zhu, Y. Yu, Realization of dark state in a three-dimensional transmon superconducting qutrit, Appl. Phys. Lett. **107**, 202601 (2015).

[51] Z. X. Zhang, P. Z. Zhao, T. H. Wang, L. Xiang, Z. L. Jia, P. Duan, D. M. Tong, Y. Yin, and G. P. Guo, Single-shot realization of nonadiabatic holonomic gates with a superconducting Xmon qutrit, New J. Phys. **21**, 073024 (2019).

[52] G. K. Brennen, G. Pupillo, E. Rico, T. M. Stace, and D. Vodola, Loops and Strings in a Superconducting Lattice Gauge Simulator, Phys. Rev. Lett. **117**, 240504 (2016).

[53] S. D. Bartlett, G. K. Brennen, and A. Miyake, Robust symmetry-protected metrology with the Haldane phase, Quantum Sci. Technol. **3**, 014010 (2018).

[54] M. A. Rol, F. Battistel, F. K. Malinowski, C. C. Bultink, B. M. Tarasinski, R. Vollmer, N. Haider, N. Muthusubramanian, A. Bruno, B. M. Terhal, and L. DiCarlo, Fast, High-Fidelity Conditional-Phase Gate Exploiting Leakage Interference in Weakly Anharmonic Superconducting Qubits, Phys. Rev. Lett. **123**, 120502 (2019).

[55] A. Kuhn, M. Hennrich, T. Bondo, and G. Rempe, Controlled generation of single photons from a strongly coupled atom-cavity system, Appl. Phys. B **69**, 373 (1999).

[56] H. Xiong, M. O. Scully, and M. S. Zubairy, Correlated Spontaneous Emission Laser as an Entanglement Amplifier, Phys. Rev. Lett. **94**, 023601 (2005).

[57] A. Kuhn, M. Hennrich, and G. Rempe, Deterministic Single-Photon Source for Distributed Quantum Networking, Phys. Rev. Lett. **89**, 067901 (2002).

[58] M. Pechal, L. Huthmacher, C. Eichler, S. Zeytinoğlu, A. A. Abdumalikov Jr., S. Berger, A. Wallraff, and S. Filipp, Microwave-Controlled Generation of Shaped Single Photons in Circuit Quantum Electrodynamics, Phys. Rev. X **4**, 041010 (2014).

[59] M. Bartkowiak, L.-A. Wu, and A. Miranowicz, Quantum circuits for amplification of Kerr nonlinearity via quadrature squeezing, J. Phys. B **47**, 145501 (2014).

[60] T. Kiss, U. Herzog, and U. Leonhardt, Compensation of losses in photodetection and in quantum-state measurements, Phys. Rev. A **52**, 2433 (1995).

[61] M. A. Nielsen and I. L. Chuang, *Quantum Computation and Quantum Information* (Cambridge University Press, Cambridge, UK, 2000).

[62] M. H. S. Amin, Consistency of the Adiabatic Theorem, Phys. Rev. Lett. **102**, 220401 (2009).

[63] P. Ehrenfest, Adiabatische invarianten und quantentheorie, Ann. Phys. (Berlin, Ger.) **356**, 327 (1916).

[64] M. Born and V. Fock, Beweis des adiabatensatzes, Eur. Phys. J. A **51**, 165 (1928).

[65] N. V. Vitanov, A. A. Rangelov, B. W. Shore, and K. Bergmann, Stimulated Raman adiabatic passage in physics, chemistry, and beyond, Rev. Mod. Phys. **89**, 015006 (2017).

[66] K. Bergmann, N. V. Vitanov, and B. W. Shore, Perspective: Stimulated Raman adiabatic passage: The status after 25 years, J. Chem. Phys. **142**, 170901 (2015).

[67] M. L. Hu, State transfer in dissipative and dephasing environments, Eur. Phys. J. D **59**, 497 (2010).

[68] G. X. Li and Z. Ficek, Creation of pure multi-mode entangled states in a ring cavity, Opt. Commun. **283**, 814 (2010).

[69] Z. Ficeka and R. Tanaś, Entangled states and collective nonclassical effects in two-atom systems, Phys. Rep. **372**, 369 (2002).

[70] X. Zhang, C. Xu, and Z. Z. Ren, High fidelity heralded single-photon source using cavity quantum electrodynamics, Sci. Rep. **8**, 3140 (2018).

[71] S. Haroche and J. M. Raimond, *Exploring the Quantum: Atoms, Cavities and Photons* (Oxford University Press, Oxford, UK, 2006).

[72] A. Reiserer and G. Rempe, Cavity-based quantum networks with single atoms and optical photons, Rev. Mod. Phys. **87**, 1379 (2015).

[73] Y. H. Issoufa and A. Messikh, Effect of dephasing on superadiabatic three-level quantum driving, Phys. Rev. A **90**, 055402 (2014).

[74] L. B. Nguyen, Y.-H. Lin, A. Somoroff, R. Mencia, N. Grabon, and V. E. Manucharyan, Phys. Rev. X **9**, 041041 (2019).

[75] A. Somoroff, Q. Ficheux, R. A. Mencia, H. Xiong, R. V. Kuzmin, and V. E. Manucharyan, Millisecond coherence in a superconducting qubit, arXiv:2103.08578.

[76] M. Reagor, M. Reagor, W. Pfaff, C. Axline, R. W. Heeres, N. Ofek, K. Sliwa, E. Holland, C. Wang, J. Blumoff, K. Chou, M. J. Hatridge, L. Frunzio, M. H. Devoret, L. Jiang, and R. J. Schoelkopf, Quantum memory with millisecond coherence in circuit QED, Phys. Rev. B **94**, 014506 (2016).

[77] A. Blais, A. L. Grimsmo, S. M. Girvin, and A. Wallraff, Circuit quantum electrodynamics, Rev. Mod. Phys. **93**, 025005 (2021).

[78] Y. Yin, Y. Chen, D. Sank, P. J. J. O'Malley, T. C. White, R. Barends, J. Kelly, E. Lucero, M. Mariantoni, A. Megrant, C. Neill, A. Vainsencher, J. Wenner, A. N. Korotkov, A. N. Cleland, and J. M. Martinis, Catch and Release of Microwave Photon States, Phys. Rev. Lett. **110**, 107001 (2013).

[79] C. W. Gardiner and M. J. Collett, Input and output in damped quantum systems: Quantum stochastic differential equations and the master equation, Phys. Rev. A **31**, 3761 (1985).

[80] C. Gustin and S. Hughes, Influence of electron-phonon scattering for an on-demand quantum dot single-photon source using cavity-assisted adiabatic passage, Phys. Rev. B **96**, 085305 (2017).

[81] M. Baur, S. Filipp, R. Bianchetti, J. M. Fink, M. Göppl, L. Steffen, P. J. Leek, A. Blais, and A. Wallraff, Measurement of Autler-Townes and Mollow Transitions in a Strongly Driven Superconducting Qubit, Phys. Rev. Lett. **102**, 243602 (2009).

[82] C. K. Law and H. J. Kimble, Deterministic generation of a bit-stream of single-photon pulses, J. Mod. Opt. **44**, 2067 (1997).

[83] J. A. Mlynek, A. A. Abdumalikov, C. Eichler, and A. Wallraff, Observation of Dicke superradiance for two artificial atoms in a cavity with high decay rate, Nat. Commun. **5**, 5186 (2014).